Volume Graphics (2007)
H. - C. Hege, R. Machiraju (Editors)

Efficient Ambient and Emissive Tissue Illumination using Local Occlusion in Multiresolution Volume Rendering

Frida Hernell[†], Patric Ljung[‡] and Anders Ynnerman[§]

Center for Medical Image Science and Visualization, Linköping University
Visual Information Technology and Applications, Linköping University

Abstract

This paper introduces a novel technique to compute illumination for Direct Volume Rendering. By adding shadow effects to volume rendered images, the perception of shapes and tissue properties can be significantly improved and it has the potential to increase the diagnostic value of medical volume rendering. The integrated intensity of incident light for a voxel is computed using a local approximation of the ambient occlusion, thus avoiding the rendering of tissues with very low illumination. Luminous tissue effects are also introduced to enhance the illumination model, controlled through an emissive component in the transfer function. This effect allows the user to highlight specific structures and can give a better understanding of tissue density. Multiresolution volume management and GPU-based computation is used to significantly speed-up the calculations and to support large data sets. The scheme yields interactive frame rates for incrementally refined ambient and emissive illumination for arbitrary transfer function changes.

Categories and Subject Descriptors (according to ACM CCS): I.3.3 [Computer Graphics]: Viewing algorithms; I.3.7 [Computer Graphics]: Color, shading, shadowing, and texture; I.4.10 [Image Processing and Computer Vision]: Volumetric;

1. Introduction

Interaction with patient specific Computed Tomography (CT) data through direct volume rendering (DVR) has become an invaluable tool in medical diagnosis and has contributed to the spread of radiological methodology into new areas of medical practice, such as the recently introduced concept of virtual autopsies in forensic medicine [LWP*06]. To further promote the use of DVR in medicine, new rendering methods that more efficiently and intuitively lead the user to areas of interest while maintaining the integrity of the visual data representations are needed. One area of development that shows promise in supporting this is the inclusion of more sophisticated lighting models that provide visual cues to enhance the perception of shapes and depth. Langer et al. [LB99] found that ambient lighting in particular, like lighting on a cloudy day, significantly enhances the ability of humans to distinguish objects and their properties.

A commonly used lighting approximation in volume rendering applications is the diffuse Phong shading model [Pho73] used in combination with the Blinn model [Bli77]. This approach is suitable for direct volume rendering since it can be readily evaluated at interactive frame rates. The method does, however, depend on the normalized gradient of the volume scalar field which limits its applicability. For instance, if the scalar data is noisy the gradients become indistinct. Another problem is that the gradients are only well defined in sharp transitions between different scalar values which means that light values can be estimated for surfaces but not as easily for homogeneous regions. In semi-transparent regions it is therefore difficult to accurately define a light approximation.

More advanced lighting models that add a higher level of realism and include self-shadowing can enhance the representation of features of the data but global illumination models are computationally expensive and cannot, today, be used

[†] frihe@cmiv.liu.se
[‡] plg@itn.liu.se
[§] andyn@itn.liu.se

in interactive DVR. A further disadvantage of such models within the context of medical visualization, is that regions of a volume can be shadowed by dense objects occluding the light. The skull for example, can occlude the light so that a tumor or other feature may not be illuminated and so cannot be identified.

Both of these problems, performance and occlusion, can be addressed through the use of a Local Ambient Occlusion (LAO) model that only considers shadowing by structures in the immediate vicinity of each voxel. The LAO method presented in this paper considers the illumination around each point in the volume. For each voxel a volumetric light source is defined, filling a spherical region arround the voxel, forming a local lighting neighborhood. A number of rays are then cast from the voxel to sample the local light contribution from this spherical region and so capture the local occlusion effects.

This paper also presents a method to include emissive tissue illumination effects in the local occlusion shading. An emissive component in the TF is used to control the luminosity of each associated data value, allowing specific data values to illuminate their immediate vicinity. The light and shadow effects gained with this technique can help the user to extract more information from the data by highlighting specific tissue types and their densities in a CT or MRI data set, for example small bullet fragments.

Estimation of local ambient occlusion is computationally demanding since it must be evaluated for each voxel. A multiresolution framework is therefore used to reduce the amount of computation in empty or homogenous spaces. Since the ambient occlusion is view independent, a re-estimation of the integrated light intensities need only be performed when the transfer function (TF) is modified. The main contributions of this paper are:

- an efficient local occlusion method for direct volume rendering using a multiresolution data structure supporting interactive frame rates
- a method for interactive TF-based emission that improves the visibility of user-specified data ranges

The remainder of this paper is organized as follows: Section 2 gives an overview of the related work in this research field with a brief introduction to the theory of ambient occlusion. Section 3 then presents the theory of the developed illumination method followed by implementation details in section 4. The results of the presented method are illustrated in section 5 and the last section summarizes the method and outlines future work.

2. Related Work

Computing self shadowing in volume rendering is a computationally demanding problem and several approximation schemes have been proposed to achieve interactive frame rates. One approach is to pre-process the light computation and store the intensities in a shadow map (see, for example, [BR98, HKSB06]). This shadow map must, however, be re-estimated each time the transfer function or light condition changes. If an update of the light map takes too long it could cause problems in clinical situations where fine-tuning of the TF is needed. Another approach, presented by Kniss et al. [KPHE02], estimates the shadows in parallel with the final volume rendering using half-angled texture slices. The half-angle refers to the angle between the light direction and the view direction. This method also includes scattering and color bleeding effects. The method however, relies on rendering based on texture slicing and supports only one light source. A variation of this method that takes several samples in the 2D shadow buffer of each slice to create dilated shadows in the light direction was presented by Desgranges et al. [DEP05]. The estimated shadow value of a voxel is, in this approach, the minimum value of the neighboring shadow values which also gives an effect of attenuation of light within an object. This method is also still limited to one light source.

The local volumetric shadowing effect presented in this paper, is comparable with ambient occlusion for surfaces, which is a simplification of the obscurance illumination model [ZIK98, IKSZ03] where incident light at a surface element is estimated by integrating the visibility over a hemisphere. A number of methods have been presented for surface rendered ambient occlusion, for example [TCM06, Ste03, SA07, SSZK04]. One of these is the vicinity shading, presented by Stewart [Ste03], who modified the rendering equation presented by Kajiya [Kaj86] to yield an illumination model, that for each surface point, estimates the light that arrives from a large number of directions. One downside of this method is long pre-processing times. Tarini et al. [TCM06] subsequently refined this model to increase the performance. Wyman et al. [WPSH06] uses a combination of Monte Carlo pathtracing and a spherical harmonic representation to approximate the irradiance over a hemisphere and allow dynamic environmental lighting. A recently presented method for surface rendered ambient occlusion [SA07] uses a low frequency model of the geometry in combination with the original geometry for a better approximation of the ambient lighting. Methods for ambient occlusion are often referred to as 'all-or-nothing' methods, which means that there is no consideration of transparency. The incoming light from a direction is blocked by any voxel with higher density along the ray. When generalizing these methods to take participating media into account, care must be taken to reduce the complexity introduced by large regions of semi-transparent voxels.

This paper also presents rendering with luminous effects. Previous examples of luminous volumes can be found in rendering of astrophysical simulations [MHLH05, KWAH06]. In those papers the emittance is estimated from physical properties such as temperature and gas density. In most cases

the luminosity of the volume is pre-computed and gives a static contribution to the illumination.

3. Volumetric Ambient Occlusion

In many applications of volume rendering it is not desired to create a realistic global illumination where objects can be fully shadowed. A local model is therefore proposed, where a limited spherical neighborhood, Ω, around each processed voxel is evaluated. To consider semi-transparent materials the local ambient occlusion model needs to go beyond the all-or-nothing approach used in previous work. The proposed technique includes semi-transparent objects and supports a smooth fading of shadows as occluding objects occupy more or less of the local neighborhood. The scheme is based on sampling the locally occluding material along multiple rays originating from the voxel at the center of Ω.

The incident light intensity, $I_k(x)$, arriving at a voxel location, x, from one ray direction, k, is given by the equation:

$$I_k(x) = \int_a^{R_\Omega} \frac{1}{R_\Omega - a} \exp(-\int_a^s \tau(u)du)ds \qquad (1)$$

where a is an initial offset from the voxel along the ray and R_Ω is the radius of the spherical support. The attenuation of the light contribution along the ray is estimated using the optical depth, the integral of transfer function densities, $\tau(s)$. Numerical evaluation of the integral in equation 1 is obtained as:

$$I_k(x) = \sum_{m=0}^{M} \frac{1}{M} \prod_{i=0}^{m-1} (1 - \alpha_i) \qquad (2)$$

in a front-to-back compositing scheme, where M is the number of samples along the ray and α_i is the sample's opacity according to the current transfer function.

As can be noted from equations 1 and 2, light is contributed at each sample point, normalized to sum to one. This ensures that shadows from an occluding object increase smoothly as a larger fraction of the ray penetrates the occluding object. Additionally, the method becomes less sensitive to the number of rays used to discretize Ω. The effect of the softer penumbra towards the edge of the strong shadow region is shown in figure 1. The local ambient occlusion for a voxel, $I(x)$, is then given by the sum of all incident light rays I_k (equation 3). An ambient bias can be specified to adjust the amount of minimum lighting. A ray is also associated with a weight, w_k in the range [0..1], and thus enables directional weighting of the ambient light.

$$I(x) = I_{\text{bias}} + \frac{1}{K} \sum_{k}^{K} w_k I_k(x) \qquad (3)$$

Estimation of the volumetric LAO is performed incrementally, updating one ray per frame, as an initial step of the rendering pipeline. The resulting light intensity of each voxel is stored in an intensity map which is used in the final volume rendering to illuminate each sample. Recomputation is only nesessary in the case of a transfer function change.

Figure 1: *Sharp shadows appear if light is contributed only at the boundary of Ω (left). This effect is avoided if light is contributed at each sample point (right).*

3.1. Emissive Tissues and Local Ambient Occlusion

Having established a framework for volumetric local ambient occlusion we can proceed to incorporate emissive components from the transfer function. This simulates single light scattering of luminous objects within the volume. Equation 1 is simply modified to also incorporate colored light emission, c_{E}.

$$I_k(x) = \int_a^{R_\Omega} \frac{1 + c_{\text{E}}(s)}{R_\Omega - a} \exp(-\int_a^s \tau(u)du)ds \qquad (4)$$

The emittance of a sample point along a ray within Ω can therefore affect the intensity and color of point x. The emissive parameter is also included during the final ray-casting, further enhancing the effect of luminosity.

4. Implementation

A volume in the transfer function domain commonly contains large areas of empty or homogenous space in which it is unnesseceary to estimate detailed illumination. Superfluous sampling in areas of low occlusion contribution can be avoided by introducing a multiresolution approach. In this implementatoin a flat multiresolution blocking method is used, as presented in [LLYM04], which allows for a graceful data reduction using the transfer function to optimize the resulting image quality. This section provides a brief review of the flat multiresolution blocking method and a detailed description of the LAO pipeline.

4.1. Flat Multiresolution Blocking

In a preprocessing stage the volume is blocked into small cubes, 16^3 voxel blocks, and organized into a multiresolution representation such that an arbitrary LOD selection can be efficiently loaded in run-time. The LOD selection is made by optimizing the resulting image quality through the

blocks' content in the TF domain and can be interactively updated. The resolution levels are discrete numbers in the range $[0..\lambda_h]$, where λ_h is the highest resolution, which is 4 in this implementation. All these blocks of different resolutions are packed into a single 3D texture accompanied with an index texture specifying the location and resolution of the blocks in the packed texture, as described in more detail in [LLY06].

The LAO computation needs an additional index texture for reverse mapping which presents a minor challenge since the location of a voxel in the volume must be determined. Potentially a block could be represented by a single voxel in the packed texture which would require a reverse index map of the same size as the packed texture itself. This is avoided by ignoring reverse mapping of blocks below a certain minimum resolution level. By ignoring blocks with the two lowest resolution levels, 1^3 and 2^3, the size of the reverse index map can be reduced by a factor of 64. All empty blocks are assigned the lowest resolution or ignored entirely and the remaining blocks are assigned higher resolutions, with a minimum of 4^3 voxels. The reverse map can then hold a block's location in volume coordinates (V) for all non-empty blocks.

4.2. Multiresolution LAO Pipeline

The LAO computation is driven by the processing of each voxel in the volume. Since a multiresolution volume management is applied, the gained data reduction from the LOD selection also implies a speed-up of the LAO processing. The LAO illumination is computed with the same data reduction as the LOD selection of the volume. The processing of each voxel can, in turn, be further accelerated by adapting the sampling rate depending on the voxel's block resolution level. This per-fragment processing pipeline is presented next and illustrated in figure 2.

The pipeline is executed for all voxels in a slice of the packed volume texture in parallel. A 3D texture is created to hold the emissive color and the ambient occlusion of each voxel. The entire volume is then processed by mapping all the slices, one-by-one, as a rendering target of a framebuffer object. The fragment pipeline is initiated by rendering a large quad over the entire framebuffer, where each pixel maps to one voxel in the mapped 3D texture. This approach is efficient but requires that the hardware support the attaching of a slice of a 3D texture to a framebuffer, as available in the latest GPU hardware generation, e.g. Nvidia GF8800 Ultra.

The fragment location, along with a per-slice constant z-position, is used to look up the corresponding voxel location in the volume through the reverse index texture, P→V. The pipeline then iterates over all the incident light directions in Ω, one direction per frame, until all the rays are processed. The number of rays, K, to sample can be dynamically configured and the ray directions are stored in a texture together with the directional weight, w_k. Ray directions are created

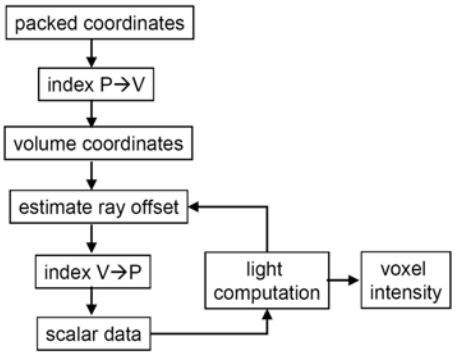

Figure 2: *Per-fragment computations to evaluate LAO for a voxel. The packed coordinates (P) are transformed to volume coordinates (V). Rays are generated to sample the volume around the voxel. For each sample the reverse index texture gives locations in the packed volume. The final fragment intensity is the average of the ray intensities.*

by subdividing a tetrahedron, icosahedron or octahedron to different levels, depending on the desired number of rays. The light contribution of a ray is blended with the previously stored value in the 3D texture, which results in an incrementally improved effect of the LAO in the rendered image. The final rendering is performed with ray casting using adaptive sampling, as described in [Lju06]. Interblock interpolation is optional in the final rendering but is not considered in the LAO computations, since it would require too many texture look ups. Artifacts due to this limitation have not been noticed.

The sampling along a ray starts at a user-defined offset, a. In addition the sampling density, d, and radius, R_Ω, of Ω can be specified. The initial offset avoids unnecessary self-occlusion for voxels on the boundary of highly opaque regions. The sampling density is adjusted for voxels in lower resolution blocks. Additional speed-up of the LAO computations can be gained by adjusting the sampling density for voxels in lower resolution blocks. In this implementation the sample distance, the step length, is increased by $(2^{\lambda_h}+2^{\lambda})/2$, for all block levels λ. Thus, the sampling rate stays fixed relative to the sampling density of the underlying volume data. Too large difference in step length leads to block artifacts. When the sampling rate changes the opacities and colors have to be corrected as well, this is done on the fly using the opacity correction formula, equation 5. To further control the effect of LAO, opacity can be modified according to a user controlled parameter, γ.

$$\alpha_{\text{modified}} = 1.0 - (1.0 - \alpha_{\text{original}})^{\gamma d \frac{2^{\lambda_h}+2^{\lambda}}{2}}. \qquad (5)$$

5. Results

All of the results presented in this paper have been generated using an implementation of the described methods on

(a) *Diffuse Illumination (26.4 FPS)* (b) *LAO with 1 direction (27.2 FPS)* (c) *LAO with 8 directions (27.2 FPS)*

Figure 3: *The left image shows diffuse illumination while the other two show local ambient occlusion using a single ray directed at the single light source (middle) and 8 rays (right). The LAO approach generates convincing shadowing effects giving a superior 3D appearance. Frame rates are given for the final rendering of the volume for a viewport of* 1024^2. *The LAO map in (b) and (c) is computed in 51.2 ms/ray, for a volume of 512x256x256 voxels at a data reduction of 4.9:1.* $R_\Omega = 1$ *block.*

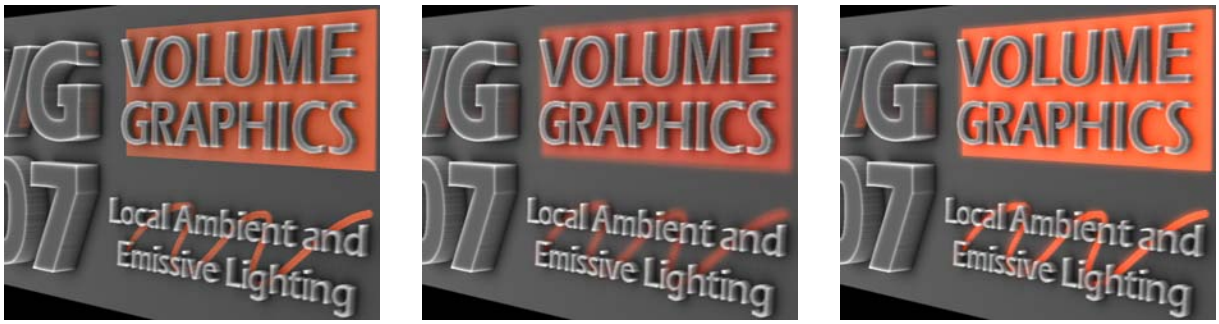

Figure 4: *Emissive illumination effects. Left to right: Emissive light captured in the ray-casting stage, emitted light illuminating the surrounding material, and both effects combined.*

a standard PC equipped with an Nvidia GeForce 8800 Ultra graphics board with 768 MB of graphics texture memory.

The series of images in figure 3 show a comparison betweeen different shading techniques using a simple synthetic data set with sharp gradients present between the 'tissues' and a variety of shapes from sharp corners to smooth curves. The volume also contains sub-surface layers of material which can be made emissive with an appropriate TF selection. The left image shows the effect of simple diffuse lighting, which provides clues about object shape and gives a sense of 3D. The image including a single occlusion sampling ray in the direction of the light source, shown in the middle, immediately shows the positive effect in terms of creating strong shadows and a stronger 3D effect. The right image show the effect of a more detailed approximation of the LAO with 8 ray directions used. The shadows are softened and more ambient lighting is included so that only deeper and sharper corners are strongly shadowed. In figure 4 the same synthetic data set is used to show the effect of the emissive lighting function applied within the rendering. In the first image we consider only the effect of the emissive material on the ray-casting pass and the LAO does not take into account the light emitted by the emissive material. Thus the emitted light is not permitted to illuminate its environment. In the second the LAO includes the emitted light and

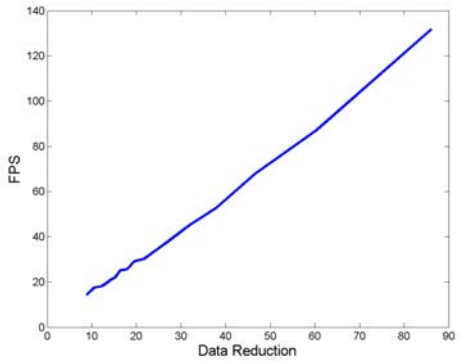

Figure 5: *Graph of the LAO computation time per ray versus data reduction. The performance of the LAO computation is super-linear with respect to the data reduction.* $R_\Omega = 1$ *block and* $M = 15$ *for* λ_h.

so the shadows are reduced in regions where emissive material is nearby. The final image shows the combined effect of emissive material both in the ray-casting pass and in the LAO.

The illumination model is based on two main approximations which have been tested for visual errors and for performance improvement. The first is the data reduction applied.

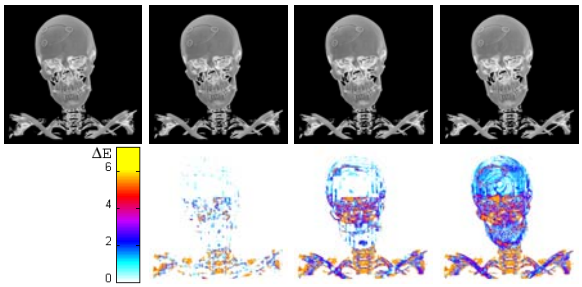

Figure 6: *Error images showing artefacts arising at different data reduction levels. The images, left to right, show 8.5:1 data reduction and 15.7:1, 31.4:1 and 92.8:1 data reduction with accompanying relative error images in the bottom row.*

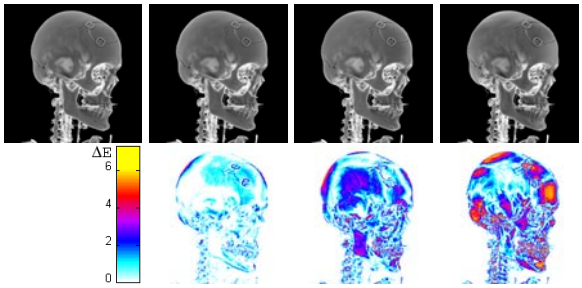

Figure 7: *Error images showing artefacts incurred when fewer ray directions are considered. The images, left to right, show 128 directions and 64, 16 and 8 directions with accompanying relative error images in the bottom row.*

Figure 5 shows the performance in frames per second (FPS) at various levels of data reduction for a volume with a native resolution of 512^3 voxels. In this case a complete LAO map is estimated for one ray, which corresponds to the calculations needed during an incremental LAO update, independently of the number of rays in which Ω is descretized. The performance increase of the LAO map creation is superlinear in the level of data reduction since the reduction increases the number of low-resolution blocks present in the volume with two contributing effects.The first is that the number of voxels is decreased and so less occlusion calculations are required, the second that low-resolution blocks permit a longer sample step and so the average time per occlusion calculation is reduced. Error measurements have been carried out, using the approach described in [LLYM04], in order to explore the impact of the data reduction. Three levels of data reduction have been choosen, from the setup in figure 5, to be evaluated. The mean of the errors (ΔE) in images rendered with data reduction 15.7:1, 31.4:1 and 92.8:1, relative to a reduction of 8.5:1, are 0.6, 1.2, and 1.6 percent, respectively (fig. 6).

The loss of accuracy when reducing the number of rays in the LAO computation is also tested with the error measurement. The errors in images rendered with 64, 16 and 8 ray directions, relative to that obtained when 128 ray directions are used, are shown in the error images in figure 7. The errors are clearly quite small, with means of 0.3, 0.7 and 0.9 percent for 64, 16 and 8 directions, respectively.

The enhancements in renderings due to the local ambient occlusion can make it much easier to distinguish the relative position of complex three dimensional shapes in volumetric data. The images shown in figure 8 show how the LAO makes clear the complex shape of the blood vessels and their position relative to the skull surface. It also enhances the visibility of the skull structure itself. Even the perception of the skull density can be improved (fig. 9).

The effects of the emissive material within a medical volume can be seen in figure 10 where a rendering of a virtual autopsy case is shown. In these images the bullet and the many fragments, which are so crucial to the forensic scientist, are not clear in the standard diffuse ray-cast image on the left but the LAO renderings with emissive material (middle) clearly show these foreign bodies as well as revealing the bone structure much more clearly. The emissive material approach compares well with the dual TF technique introduced in [LWP*06] to highlight similar foreign bodies. Combining LAO and diffuse shading (right) can, in some applications, intensify the perception of shapes.

6. Conclusions and Future Work

In this paper we have presented a method for inclusion of local ambient and emissive lighting for volume rendering applications. The results show that improved perception of local features in the volume can be obtained. Since the illumination model does not rely on gradients, it could also prove beneficial for noisy data sets such as 3D ultrasound.

The limitation of the ambient occlusion to a local neighborhood, combined with a multiresolution framework, enables rendering at interactive speeds, a delay only being introduced by the recalculation of the occlusion volumes when transfer functions are changed. The local ambient occlusion model has also been extended to include emissive lighting from selected tissues in the volume. This enables the user to emphasize features of interest, increasing the visual acuity of the regions around emissive voxels.

The developed methods have been tested by radiologists who considered the methods to be very promising. Further evaluation through a comprehensive user study is needed, however, to explore the potential of these approaches for medical volumes. We also foresee many possible further developments. Directional ambient occlusion could yield very distinct shadows and allowing the user to interactively alter the shadowing would further improve the depth perception. This would, in turn, call for faster recalculation of the illumination parameters after changes in the light direction. Another area of interest is the connection of emission with tissue classification methods to further improve the detection of regions of interest such as blood vessels or tumors.

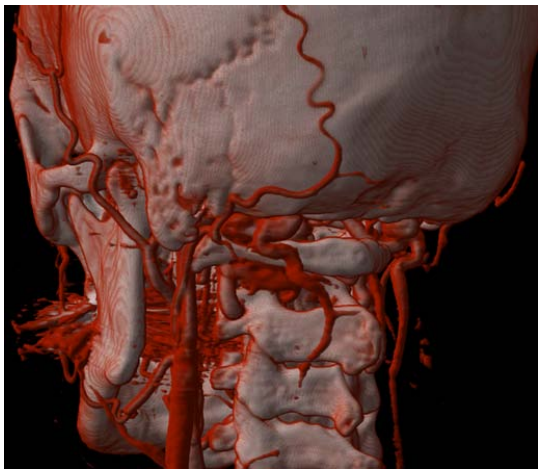

(a) Diffuse Illumination

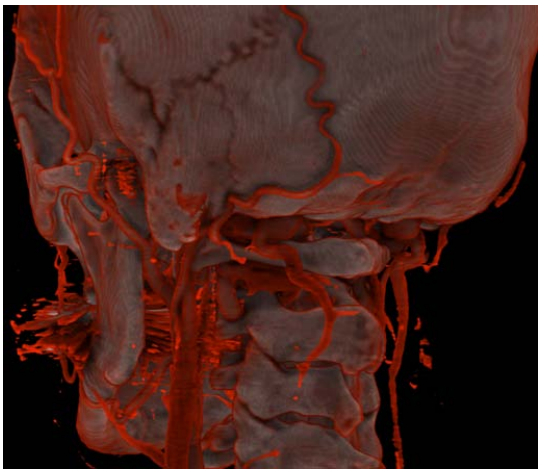

(b) Local Ambient Occlusion, 32 rays

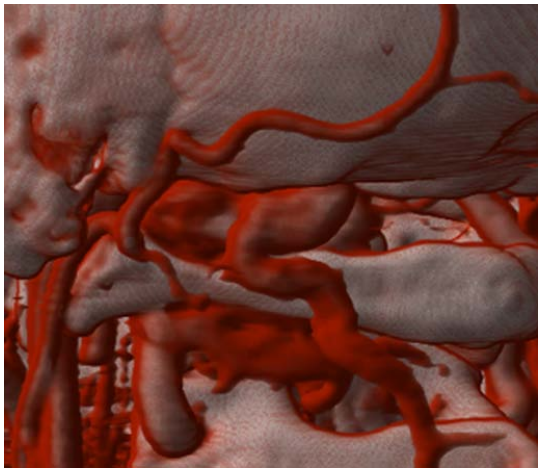

(c) Close-up of vessels in (a)

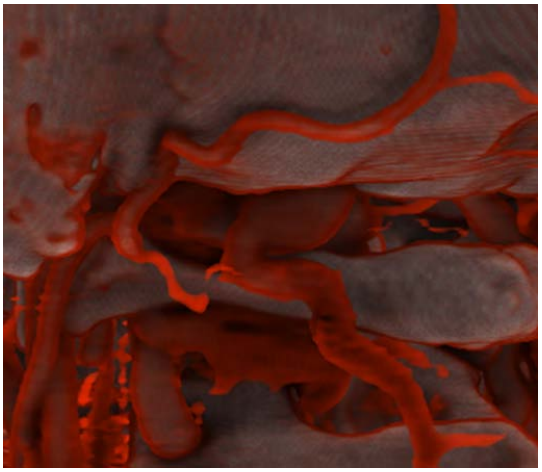

(d) Close-up of vessels in (b)

Figure 8: *Example images showing the enhanced 3D structure made clear through the LAO method. $R_\Omega = 2$, $a = 0.8 \cdot d$ and $d = 1/16$ for λ_h.*

Figure 9: *The density of the skull appears better with LAO (right) compared to diffuse shading (left). $R_\Omega = 1$ block. The LAO method is not sensitive to gradient data which can be an advantage for noisy data sets. However, a combination of LAO and diffuse shading can in some situations be favourable in order to explore fine structures, as in figure 10.*

Acknowledgements

This work has been funded by the Swedish Research Council, grant 621-2004-3829, and the Strategic Research Center MOVIII, founded by the Swedish Foundation for Strategic Research, SSF. The medical data sets used are provided by Siemens and the Center for Medical Image Science and Visualization (CMIV). Many thanks to co-workers at the division for Visual Information Technology and Applications.

References

[Bli77] BLINN J. F.: Models of light reflection for computer synthesized pictures. *SIGGRAPH Computer Graphics 11*, 2 (1977), 192–198.

[BR98] BEHRENS U., RATERING R.: Adding shadows to a texture-based volume renderer. In *IEEE Symposium on Volume Visualization* (1998), pp. 39–46.

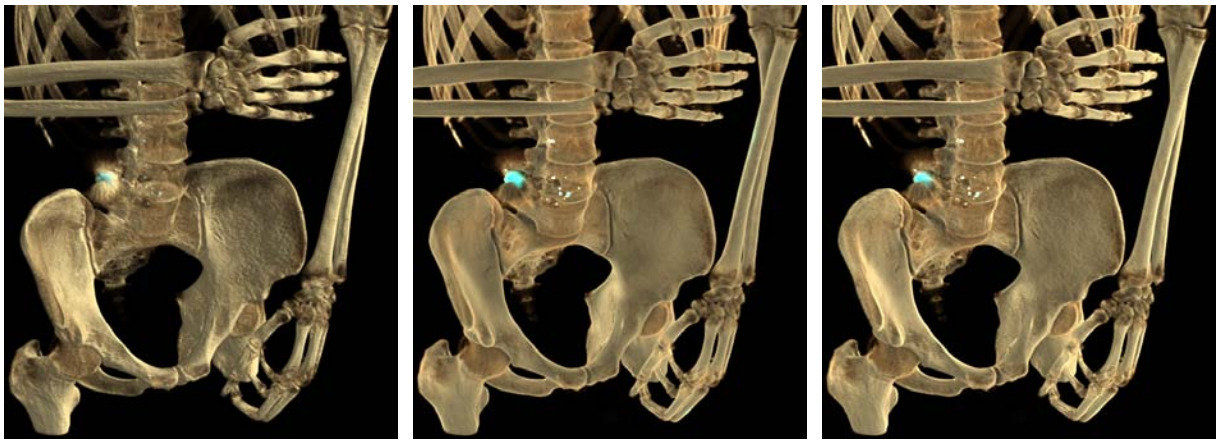

(a) Diffuse Illumination *(b) LAO with emission* *(c) Diffuse Illumination × LAO (with emission)*

Figure 10: *Example images showing the enhanced information from the emissive materials. The bullet and fragments are clearly visible in the abdomen. The effect of the LAO in revealing the bone structure is also very clear. A combination of LAO and diffuse shading intensifies fine details, for example the structure on the pelvis.*

[DEP05] DESGRANGES P., ENGEL K., PALADINI G.: Gradient-free shading: a new method for realistic interactive volume rendering. In *Proceedings of Vision, Modelling, and Visualization* (Nov. 2005). Berlin, Akademische Verlagsgesellschaft Aka GmbH.

[HKSB06] HADWIGER M., KRATZ A., SIGG C., BÜHLER K.: GPU-accelerated deep shadow maps for direct volume rendering. In *Proceedings of Eurographics/SIGGRAPH Graphics Hardware* (2006), pp. 49–52.

[IKSZ03] IONES A., KRUPKIN A., SBERT M., ZHUKOV S.: Fast, realistic lighting for video games. *IEEE Computer Graphics and Applications 23*, 3 (May 2003), 54–64.

[Kaj86] KAJIYA J. T.: The rendering equation. In *Computer Graphics (Proceedings of Siggraph 86)* (New York, NY, USA, 1986), vol. 20, ACM Press, pp. 143–150.

[KPHE02] KNISS J., PREMOZE S., HANSEN C., EBERT D.: Interactive translucent volume rendering and procedural modeling. In *Proceedings of IEEE Visualization* (2002), pp. 109–116.

[KWAH06] KAEHLER R., WISE J., ABEL T., HEGE H.-C.: GPU-assisted raycasting for cosmological adaptive mesh refinement simulations. In *Volume Graphics* (2006), pp. 103–110.

[LB99] LANGER M. S., BÜLTHOFF H. H.: Perception of shape from shading on a cloudy day, October 1999. Technical report, No. 73, Max-Planck-Institut für biologische Kybernetik.

[Lju06] LJUNG P.: Adaptive sampling in single pass, GPU-based raycasting of multiresolution volumes. In *Proceedings of Eurographics/IEEE Workshop on Volume Graphics 2006* (2006), pp. 39–46,134.

[LLY06] LJUNG P., LUNDSTRÖM C., YNNERMAN A.: Multiresolution interblock interpolation in direct volume rendering. In *Proceedings of Eurographics/IEEE Visualization* (2006), pp. 259–266.

[LLYM04] LJUNG P., LUNDSTRÖM C., YNNERMAN A., MUSETH K.: Transfer function based adaptive decompression for volume rendering of large medical data sets. In *Proceedings of IEEE Volume Visualization and Graphics* (Washington, DC, USA, 2004), IEEE Computer Society, pp. 25–32.

[LWP*06] LJUNG P., WINSKOG C., PERSSON A., LUNDSTRÖM C., YNNERMAN A.: Full body virtual autopsies using a state-of-the-art volume rendering pipeline. *IEEE Transactions on Visualization and Computer Graphics 12*, 5 (2006), 869–876.

[MHLH05] MAGNOR M. A., HILDEBRAND K., LINTU A., HANSON A. J.: Reflection nebula visualization. In *Proceedings of IEEE Visualization* (2005), pp. 255–262.

[Pho73] PHONG B. T.: *Illumination for computer-generated images.* PhD thesis, 1973.

[SA07] SHANMUGAM P., ARIKAN O.: Hardware accelerated ambient occlusion techniques on GPUs. In *Proceedings of Interactive 3D graphics and games* (New York, NY, USA, 2007), ACM Press, pp. 73–80.

[SSZK04] SATTLER M., SARLETTE R., ZACHMANN G., KLEIN R.: Hardware-accelerated ambient occlusion computation. In *Vision, Modeling, and Visualization* (Nov. 2004), pp. 119–135.

[Ste03] STEWART A. J.: Vicinity shading for enhanced perception of volumetric data. In *Proceedings of IEEE Visualization* (2003), IEEE Computer Society, pp. 355–362.

[TCM06] TARINI M., CIGNONI P., MONTANI C.: Ambient occlusion and edge cueing to enhance real time molecular visualization. *IEEE Transaction on Visualization and Computer Graphics 12*, 6 (Sep/Oct 2006).

[WPSH06] WYMAN C., PARKER S., SHIRLEY P., HANSEN C.: Interactive display of isosurfaces with global illumination. *IEEE Transactions on Visualization and Computer Graphics 12*, 2 (2006), 186–196.

[ZIK98] ZHUKOV S., INOES A., KRONIN G.: An ambient light illumination model. In *Rendering Techniques* (1998), Drettakis G., Max N., (Eds.), Eurographics, Springer-Verlag Wien New York, pp. 45–56.